

Contact stresses and fatigue life in a knee prosthesis: comparison between in vitro measurements and computational simulations

Tomaso Villa*, Francesco Migliavacca, Dario Gastaldi, Maurizio Colombo, Riccardo Pietrabissa

Dipartimento di Ingegneria Strutturale and Dipartimento di Bioingegneria, Laboratory of Biological Structure Mechanics, Politecnico di Milano, Piazza Leonardo da Vinci 32, Milano 20133, Italy

Accepted 23 June 2003

Abstract

The evaluation of contact areas and pressures in total knee prosthesis is a key issue to prevent early failure. The first part of this study is based on the hypothesis that the patterns of contact stresses on the tibial insert of a knee prosthesis at different stages of the gait cycle could be an indicator of the wear performances of a knee prosthesis. Contact stresses were calculated for a mobile bearing knee prosthesis by means of finite element method (FEM). Contact areas and stresses were also measured through in vitro tests using Fuji Prescale film in order to support the FEM findings.

The second part of this study addresses the long-term structural integrity of metal tibial components in terms of fatigue life by means of experimental tests and FEM simulations. Fatigue experimental evaluations were performed on Cr–Co alloy tibial tray, based on ISO standards. FEM models were used to calculate the stress patterns. The failure risk was estimated with a standard fatigue criterion on the basis of the results obtained from the FEM calculations. Experimental and computational results showed a positive matching.

© 2003 Elsevier Ltd. All rights reserved.

Keywords: Fuji film; Finite element method; Rotating platform knee prosthesis; Tibial tray; ISO standard

1. Introduction

Design of prostheses has been improved by the help of computer aided design (CAD) and structural analyses based on the finite element method (FEM). These two methods, coupled together, allow the calculation of mechanical quantities (such as stresses, deformations and contact pressures) and investigation of the different behaviour of prostheses with various designs. Such quantities can be measured also by means of in vitro tests but the advantage of CAD-FEM is the possibility of changing the geometrical and material parameters of the prosthesis and evaluating its different behaviour before manufacturing prototypes.

The evaluation of mechanical properties is fundamental for the prevention of early failure of knee prostheses: indeed, the early wear of the ultra high

molecular polyethylene (UHMWPE), which is, by now, the main cause for knee joint arthroplasty failure (Wasielowski et al., 1994; Blunn et al., 1997), is related to the extension of contact areas and to the magnitude of contact pressure.

Two main design approaches for the bearing component of total knee replacements are at the moment available on the market: the fixed one and the mobile one.

In order to achieve the complex motions of the natural knee, fixed bearing total knee replacements are obliged to incongruent contacts. Small contact areas, in conjunctions with high joint loads, favour fatigue and delamination type wear of the polyethylene (PE) (Rose and Goldfarb, 1983; Rostoker and Galante, 1979). Furthermore, the tendency for backside wear with modular tibial trays (TTs) and the loosening at the implant–bone interface are favoured where increased constraint is present.

Due to these drawbacks, the popularity of mobile bearing total knee replacements is increasing because

*Corresponding author. Tel.: +39-02-2399-4283; fax: +39-02-2399-4286.

E-mail address: villa@stru.polimi.it (T. Villa).

they potentially avoid the problems involved with the necessary trade-off between conformity and constraint of fixed bearing designs: their advantages are the theoretical reduction of contact stresses with consequent reduction of fatigue and delamination wear. Moreover, the bone–cement interface may be improved in its integrity with a mobile PE insert, which theoretically reduces constraints. Also clinical studies on the intermediate follow-up seem to encourage mobile bearing knee replacements (Buechel and Pappas, 1990; Callaghan et al., 2000; Jordan et al., 1997; Murray et al., 1998; Sorrells, 1996; Svard and Price, 2001).

On the other hand, fluoroscopic studies (Stiehl et al., 1997) found out that, in some patients, bearing motion actually does not occur, thus causing a possible alteration of the desired kinematics of the artificial joint; furthermore, the surface between the PE insert and the TT, due to their relative motion, has become a potential site for PE wear (Bell et al., 1999) and this fact has brought the necessity of investigating also the performances of this surface. In this regard, the sterilisation process may also play a role on its performances (Buchalla et al., 1995; Baker et al., 2000).

Another important issue in the performance of knee prosthesis is related to fatigue phenomena. Indeed, catastrophic failures of the tibial baseplate due to fatigue fracture have been reported in patients (Altintas et al., 1999; Abernethy et al., 1996; Maruyama et al., 1994; Mendes et al., 1984; Morrey and Chao, 1988), in consequence of loss of bony support through bone remodeling or osteolysis, severe varus or valgus deformities (Chen and Krackow, 1994) or as a result of stress-shielding in response to a prosthesis implant (Flivik et al., 1990). Tibial bone loss may also be due to the presence of a layer of fibrous tissue between the bone and cement (Scott et al., 1984). Other clinical factors affecting the prostheses performances are axial malalignment, overloading due to patient weight and/or high activity level and poor fixation of the tibial component (Abernethy et al., 1996; Mendes et al., 1984; Scott et al., 1984).

In this light tray design is an important factor, as fracture has occurred as a result of inadequate thickness, sharp corners and small radii between the tray and its rim (Abernethy et al., 1996; Mendes et al., 1984; Gradisar et al., 1989; Moreland, 1988). Lastly, the choice of material and the manufacturing process may play a significant role in determining fatigue performances of this component. In this regard, the International Standards Organisation (ISO) has proposed an endurance test (ISO 14879-1, 2000) to ensure a long-term durability of the tray.

In this paper, we compare results from two methodologies, namely the *in vitro* tests and the FEM simulations, to study: (i) the contact pressures and areas on both the superior and inferior surfaces of the

PE tibial insert at different instances of the gait cycle; (ii) the fatigue life of a TT of a mobile bearing knee prosthesis in accordance with international standard protocol.

2. Material and methods

A rotating platform total knee prosthesis made of a Cr–Co alloy femoral component (FC), a Cr–Co alloy TT and a UHMWPE insert was purposely designed and prototyped for this study: the CAD sketches were used to create the FEM models while the prototypes were built in order to carry out the experimental tests.

2.1. Contact stresses and areas

2.1.1. Experimental test

In order to measure contact areas and pressures, Fuji Prescale pressure-sensitive (FP) films were used. FP films are able to get coloured at different intensities of red depending on to the local value of pressure which are subjected to. Three different kinds of FP film were used: LLW, (measuring range 0.5–2.5 MPa), LW (measuring range 2.5–10 MPa) and MS (measuring range 10–50 MPa).

Before performing the tests, a procedure was set up to define the FP film calibration curve: from each sheet of FP film a $40 \times 50 \text{ mm}^2$ rectangle was cut and five different pressure values (included in the sensitivity range of the film) were imposed to the film using a device mounted on a MTS 858 MiniBionix testing machine (MTS Systems, Minneapolis, MN, USA). The load was measured by a MTS 662.20 D-05 load cell and imposed by a loading device of known circular section. The test temperature was set and controlled through a type-N thermocouple connected to a HP 34970 temperature indicator (Hewlett-Packard, USA). Digitized images of the prints were obtained through a HP ScanJet 6250C scanner. For each print the mean value of the colour intensity in the impressed area was calculated; this value was associated to the applied pressure, thus allowing to set one point of the calibration curve.

In order to obtain the maps of the contact pressures between the femoral condyles and the tibial baseplate, the knee prosthesis was mounted on the testing machine through a purposely made set-up (Fig. 1). Tests were performed with the FC inclined at 15° , 45° and 60° (Fig. 2).

For each flexion degree, two FP strips were positioned between each femoral condyle and the tibial PE insert and two between the PE insert and the tibial baseplate. A vertical load was then applied for 60 s: the values were 2200 N at 15° flexion, 3200 N at 45° and 2800 N at 60° in accordance with the study after Morrison (1970). The extension of contact areas was measured using a LLW

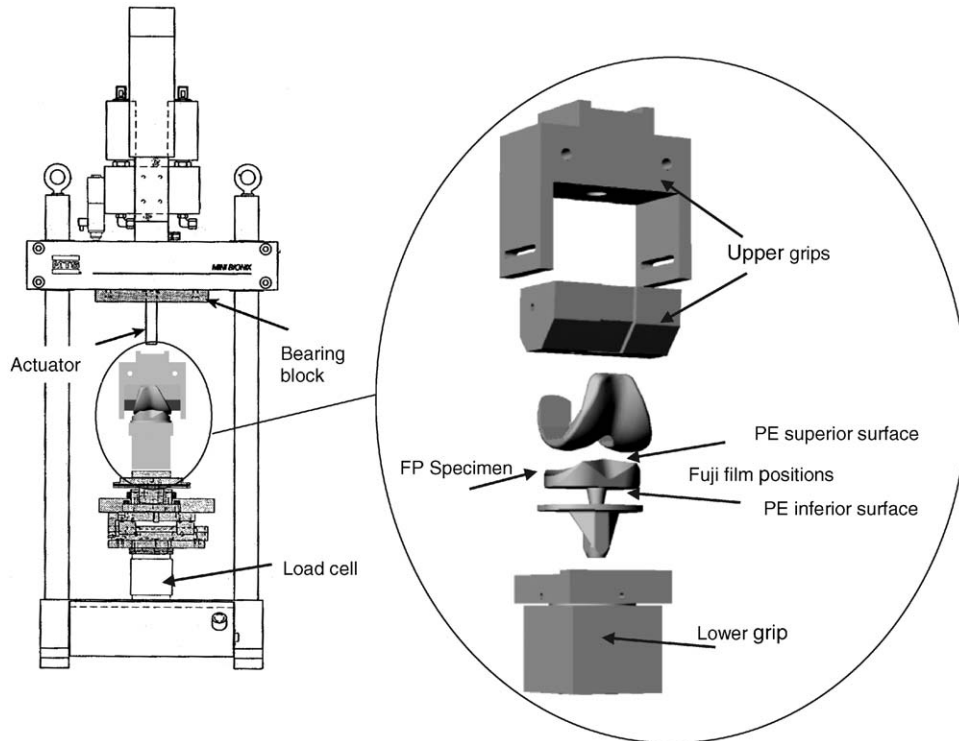


Fig. 1. Loading device for contact pressure tests.

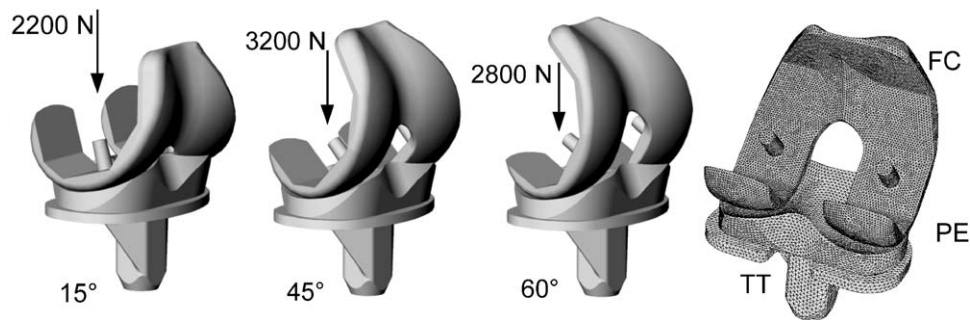


Fig. 2. The three configurations tested with the corresponding loads and a posterior view of the meshes of the FC, the PE insert and the TT.

FP film for all the configurations: the repeatability of this procedure was assessed by repeating the measurement on the superior surface three times for each flexion angle. Mean value and standard deviation were calculated. Considering that the contact area measurements on the upper surfaces are the most critical due to the curvature of the PE insert, after assessing the repeatability of this condition, the remaining contact area measurements on the lower surface and the pressure measurements were performed with only one test. Contact pressures were measured using LW or MS FP film.

One PE insert was utilised for all the tests; in order to avoid viscoelastic effects that could influence the distribution of the contact pressures and areas after each test the PE was kept unloaded for 1 h.

The contact pressure pattern was achieved as in the calibration process. A MATLAB routine able to associate a pressure value to every pixel of the image yielded the pressure colour map. The images of contact areas from LLW FP film were imported into Osiris Imaging Software by which measurements of the areas were obtained under the hypothesis of planar surfaces.

2.1.2. FEM models

A three-dimensional model of the tested mobile bearing knee prosthesis was developed (Fig. 2). It includes the FC, the PE insert and the TT. 4-node tetrahedral elements were adopted for the FC and the TT while 10-node modified tetrahedral elements were adopted for the PE insert. The grid independence of the solution was obtained by a process of refinement till a

total number of 256,705 elements and 142,708 nodes was reached. The material properties of the CoCrMo alloy consistent to the 5832-4 ISO standard used for the FC and TT were represented by an elastic constitutive law (Young modulus equal to 200 GPa and Poisson ratio to 0.3) till the yield stress (560 MPa) and through a von Mises–Hill plasticity model with kinematic hardening for the plastic region till the ultimate tensile stress σ_R (1000 MPa). The PE insert was treated as a non-linear deformable body with a Poisson ratio of 0.45 and a tangent elastic modulus governed by a fourth-order constitutive relationship with von Mises stress (σ) (Otto et al., 2001):

$$E(\sigma) = 643.92 - 12.31\sigma - 3.61\sigma^2 + 0.199\sigma^3 - 0.00283\sigma^4 \text{ MPa.}$$

As regard the boundary conditions, loads applied on the FC were equal for magnitude and direction to those adopted in the experimental tests; the TT at its inferior surface including the stem was constrained in all 6 degrees of freedom. A static coefficient of friction between the PE insert and the Cr–Co components was adopted and its value was 0.12. Simulations were performed using ABAQUS 6.2-7 (Hibbit Karlsson & Sorensen, Inc., Pawtucket, RI, USA).

2.2. TT fatigue life

2.2.1. Experimental test

Fatigue tests on the TT were performed following the ISO 14879-1 standard specification. A set-up (Fig. 3) holding the specimen as a cantilever with one-half

rigidly fixed and the other one subjected to the total loading was built in accordance with standard requirements. The specimen was fixed and supported up to its centreline by a clamping vice and the empty space under the fixed half was filled with polymethylmethacrylate (PMMA) bone cement that worked as an embedding material. In order to distribute the load, a UHMWPE spacer was positioned between the TT and a metallic spherical indenter connected to the MTS 858 Mini-Bionix actuator that worked as load applicator. Loads were measured by a MTS 661.19 F-04 load cell.

A static test was performed to obtain the load-displacement curve and the yield limit of the TT before the fatigue test.

Six specimens were tested according to ISO 14879-1. A compressive wavesine load was applied up to a 7 Hz maximum frequency: the minimum load was 0 N and the maximum load was 500, 2000 or 4000 N in accordance with the study after Ahir et al. (1999) and in order to prevent plastic deformation of the tray during the test. Fatigue tests were performed until the tibial base plate exhibited failure or until five million cycles were achieved.

2.2.2. FEM models

A three-dimensional model was adopted to simulate the above-described in vitro fatigue tests. A sensitivity analysis on the grid spacing of the TT was performed by refining a first attempt mesh (9141 nodes and 38218 elements) until independence of the numerical solution was reached with a 25,402 nodes and 115,414 elements model. A further refinement was performed in the area

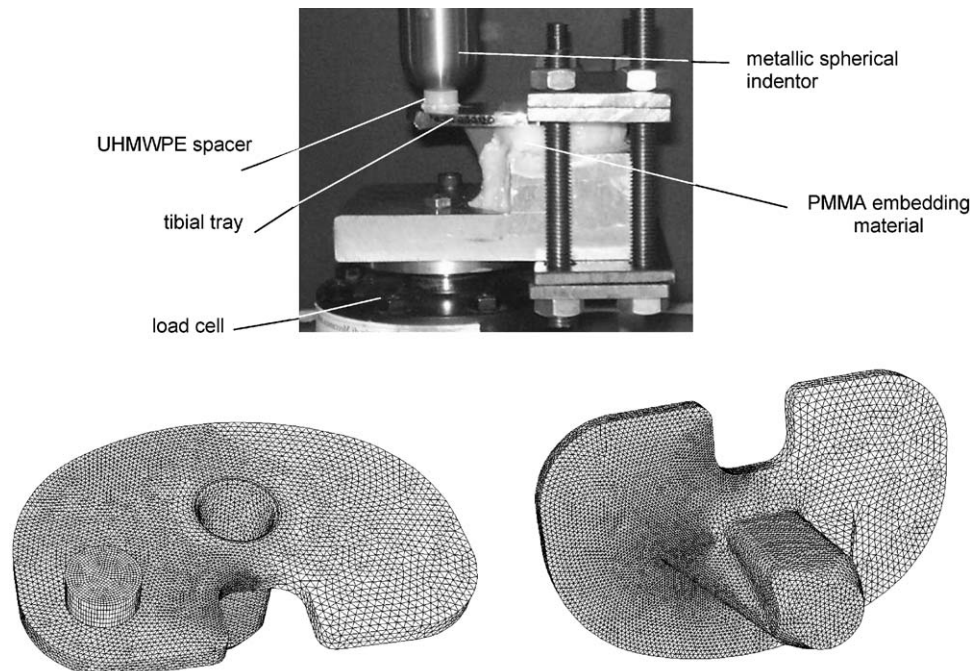


Fig. 3. Experimental set-up for fatigue test on the TT (top); meshes of the TT and the PE spacer (bottom).

where the highest stress gradient either in the superior and the inferior surfaces is expected (Fig. 3) leading to a 25,910 nodes and 109,643 elements model. The PE spacer (PEsp) was meshed with 3015 8-node-hexahedral elements. As regard the boundary conditions, on the PEsp the applied loads were equal for magnitude and direction to the maximum adopted in the experimental tests. One half of the TT in its inferior surface including half of the stem was constrained in all 6 degrees of freedom. Under the hypothesis that neither viscous nor dynamic phenomena characterise the fatigue test of the TT, the simulations were performed to calculate the stress patterns after the static application of the peak loads imposed during the in vitro tests.

The criterion proposed by Sines (1959), which is the most popular high-cycle fatigue criterion for multiaxial in-phase loads, was selected in our analysis to establish the fatigue life (N_f). Such criterion follows:

$$\sigma_{VM} + (\sigma_F/\sigma_R)I_m \leq \sigma_F, \quad (1)$$

where σ_{VM} is the alternate component of the von Mises stress calculated as half of the maximum static FEM stress, I_m is the first invariant of the mean principal stresses calculated from FEM, σ_R is the ultimate tensile strength and σ_F is the fatigue limit of the material at the number of cycle foreseen (N_f).

The fatigue life N_f was calculated combining the previous equation with the following:

$$\sigma_F = N_f^K C \quad (2)$$

which describes the analytical formulation of the Wöhler diagram in its first approximation for N_f in the interval 10^3 – 10^7 . K and C are constants, related to the fatigue limit $\bar{\sigma}_F$ and σ_R , and they can be expressed, respectively, as follows:

$$K = \log_{10}(\sigma_R/\bar{\sigma}_F)^{1/4}, \quad C = \bar{\sigma}_F^{3/4} \sigma_R^{7/4} \quad (3)$$

The values of $\bar{\sigma}_F$ were chosen from literature data (Ahir et al., 1999): the range was 250–400 MPa.

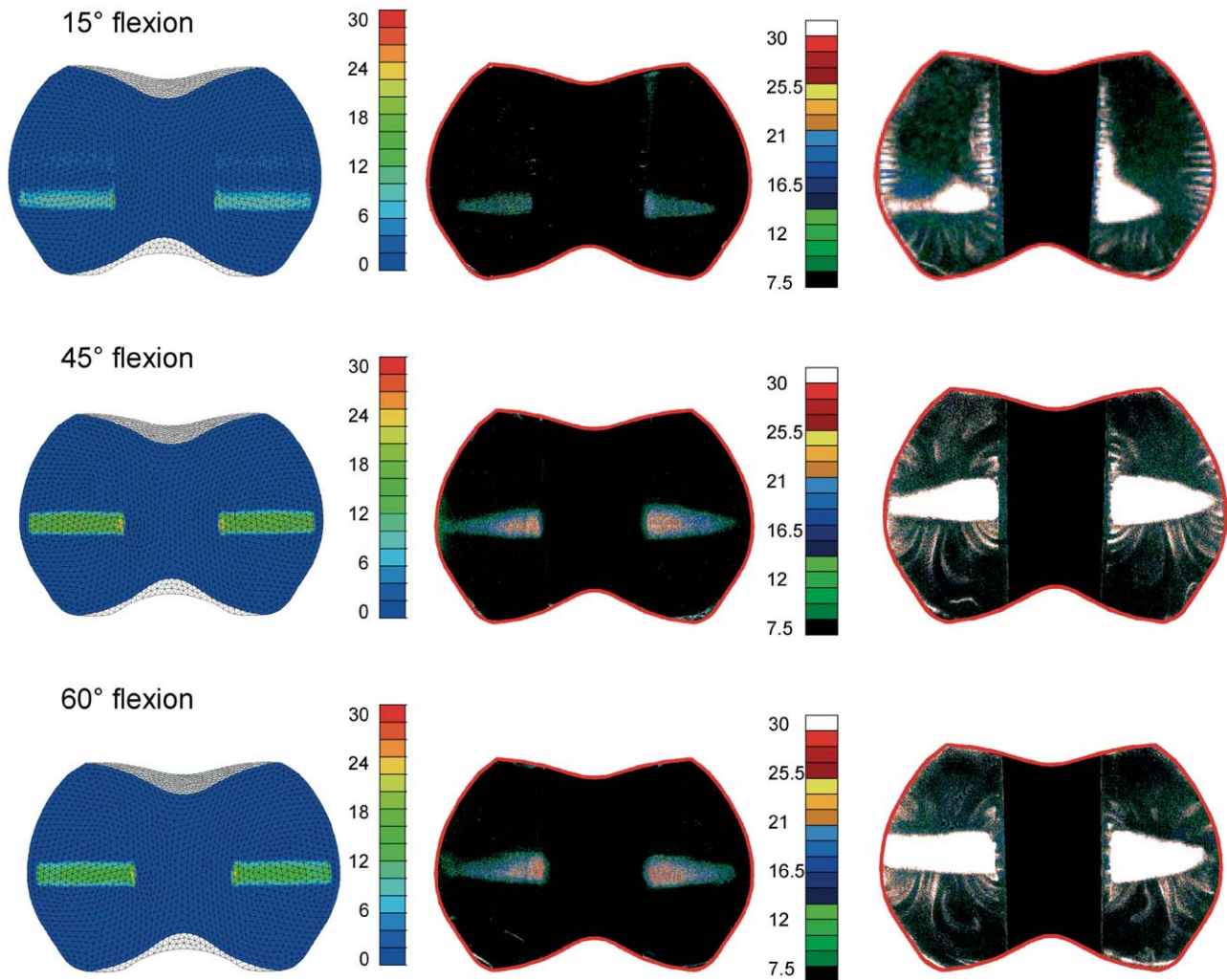


Fig. 4. Left column: contact pressure maps on the superior surface of the PE insert at 15°, 45° and 60° of flexion. Middle column: measured contact pressure maps on the superior surface. Right column: measured contact areas on the superior surface. Values in MPa.

3. Results

3.1. Contact stresses and areas

Figs. 4 and 5 report the calculated contact pressure maps as well as the measured FP maps obtained at the inferior and superior surfaces of the PE insert in the three simulated configurations. In these figures the contact areas obtained in the experimental tests are reported as well. The FP experimental procedure showed a good repeatability considering the values of standard deviation on the three measurements for each flexion angle: 2.8%, 1.9% and 4% of the mean value at 15°, 45° and 60°, respectively.

At 15° flexion, both FEM and FP maps show that the contact is not yet present in the most concave zone of the superior PE surface and that the pressure distribution is quite uniform on the whole contact area. As regards pressure values, they are similar: 15 MPa for the FEM vs. 14.5 MPa for the FP at the superior PE surface and 5 vs. 6.5 MPa at the inferior PE surface.

At 45° flexion the contact area seems to move from the posterior zone to the anterior one, corresponding to the most concave zone of the PE; moreover, the highest values of contact pressures both in the FEM model and in the FP analysis are located near the central crest, differently from the uniform distribution found at 15° flexion. The pressure values are 27.7 MPa for the FEM and 25 MPa for the FP at the superior PE surface. At the inferior surface the values are 9.6 and 11.5 MPa for the FEM and FP, respectively.

Lastly, at 60° flexion the results show a similar pattern behaviour as in the 45° configuration. The pressure values, however, are slightly lower as the load is lower than at 45° flexion. The values are 24.6 MPa for the FEM and 22 MPa for the FP at the superior surface, while at the inferior PE surface they are 8.3 and 9.5 MPa for the FEM and FP, respectively.

Fig. 6 shows a quantitative comparison of the contact areas and the maximum pressures calculated from the images of Figs. 4 and 5. As regard the contact areas the percentage difference between FEM areas and FP ones

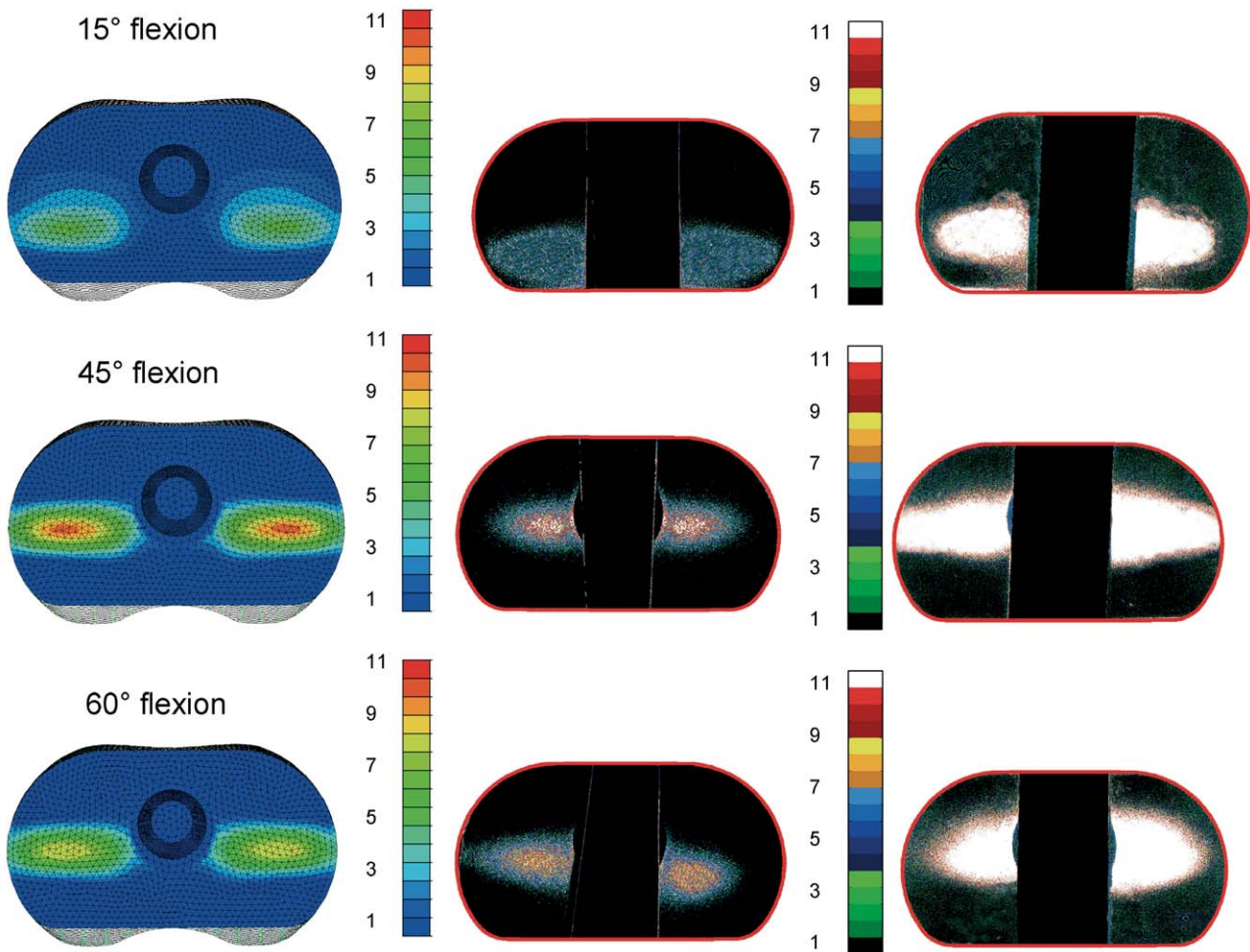


Fig. 5. Left column: contact pressure maps on the inferior surface of the PE insert at 15°, 45° and 60° of flexion. Middle column: measured contact pressure maps on the inferior surface. Right column: measured contact areas on the inferior surface. Values in MPa.

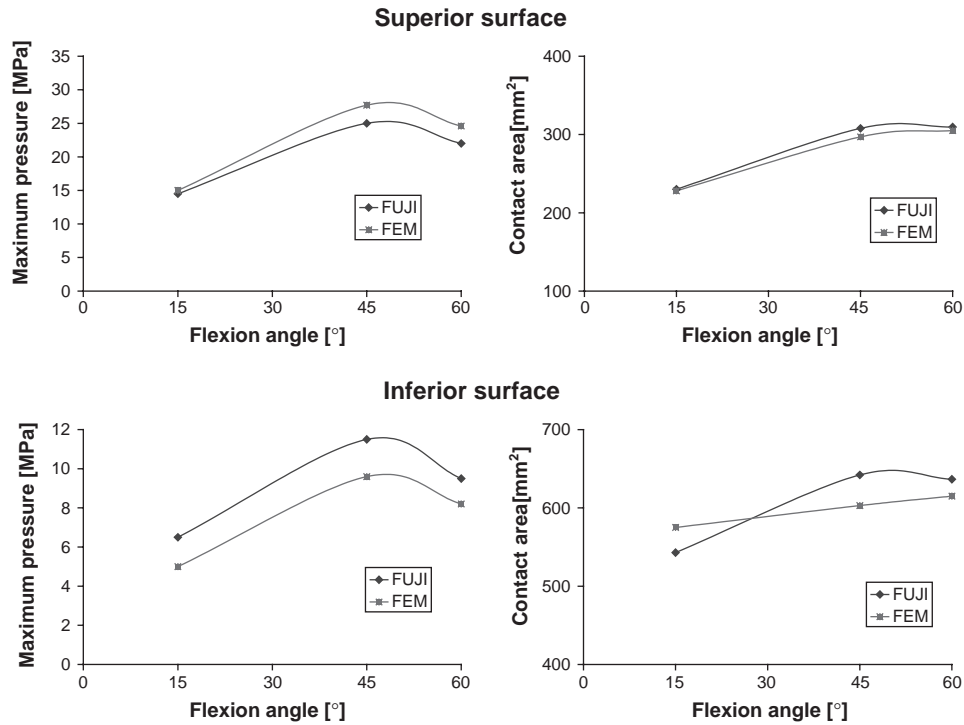


Fig. 6. Comparison of FEM simulations and Fuji measurements.

evaluated as $[(\text{FEM area} - \text{FP area}) / \text{FEM area}] \cdot 100$ is between -1% (at 15° flexion) and -4% (at 45° flexion) for the superior surface and between 6% (at 15° flexion) and -6% (at 45° flexion) for the inferior surface.

3.2. Fatigue life

Fig. 7 shows the comparison between the FEM and the laboratory tests for the static test in conjunction with the load-displacement curve obtained. From the photograph it is possible to notice that the plastic deformation area is very similar to the stress contour pattern obtained from the FEM simulation when the load is 6000 N.

From FEM simulations the alternate σ_{VM} stresses were 37, 152 and 285 MPa and the I_m stresses were 60, 240 and 345 MPa when the loads were 500, 2000 and 4000 N, respectively.

The estimated N_f for these cases were 4.2×10^4 or 5×10^5 for 4000 N load when σ_F was 250 or 400 MPa, respectively; in the case of 500 and 2000 N load the estimated N_f was greater than 10^7 for both adopted fatigue limit σ_F . At 4000 N load, the two laboratory tests produced failure at 1.7×10^5 and 3.8×10^5 cycles, respectively. Fatigue tests on the prostheses at 500 and 2000 N reached five million cycles each without any sign of failure, as predicted by the FEM simulations.

In Fig. 8 the von Mises stress contour plot for the 4000 N load configuration is depicted together with the photograph of a tested prosthesis after failure at 4000 N.

This picture shows that the failure propagated from the sites of maximum stress.

4. Discussion

The knowledge of contact pressures and areas in total knee replacements are considered as a reliable tool to predict the potential wear of PE insert (Sathasivam et al., 2001). The use of FP film to measure them has been proposed and accepted (McNamara et al., 1994) although some problems arise during the test. Indeed, FP film does not properly adapt to the curvatures of the prosthesis and its surface undergoes crimping. The use of more than one strip of smaller dimension is thus required to better follow the shape of the PE insert but this artifice yields some overestimation of contact areas and pressures due to boundary effects. Indeed, if the strip does not overlap the whole contact area, the stress distribution on the boundaries of the FP film is altered by the presence of the film itself and the microcapsules of its active layer are forced to break; the colour-developing material must thus soak a great quantity of liquid released by the microcapsules and this produces a print of greater dimension than the real contact area is. This phenomenon has been reported by Harris et al. (1999). Both the crimping of the FP film surface and the influence of boundary effects can be easily seen in the images reported in Figs. 4 and 5 of LLW contact area measurements of the superior and inferior surface of the

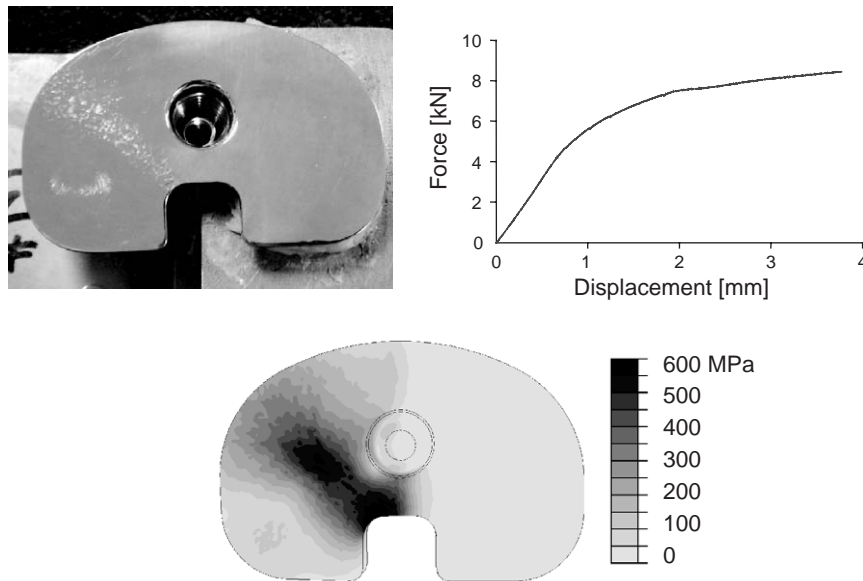


Fig. 7. Prosthesis after static test and load displacement curve (top); FEM von Mises stresses at 6000 N load.

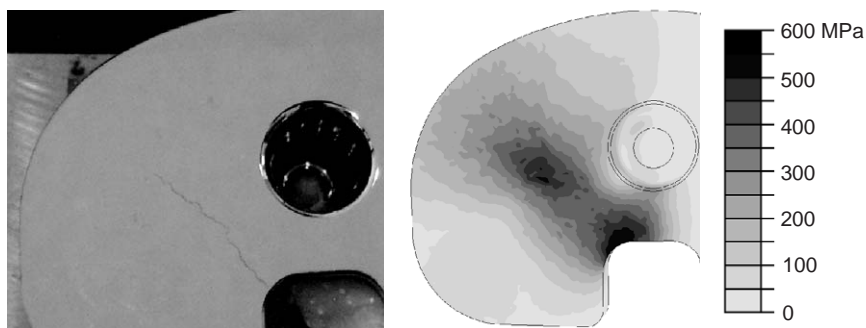


Fig. 8. Crack in the TT after fatigue test (left); von Mises contour patterns at 4000 N load (right).

PE insert. In particular, at the superior surface the contact areas are much wider toward the centre of the PE insert and tend to become thinner toward its sides; the reason is that the curvature of the PE insert is greatly enhanced near the central tibial crest and thus this is the first part of the PE insert that, during the loading process, comes in contact with the femoral condyles. As a consequence this causes a pressure overload which is responsible for the wider area towards the central tibial crest. In spite of those experimental problems, our results obtained with FP films are consistent with other authors' (Szivek et al., 1995).

In order to avoid the problems coming from the use of FP film a different methodology to calculate contact pressures and areas has been investigated: FEM have already been proposed in literature in order to calculate stresses in different designed knee prostheses (Yang and Lin, 2001; Otto et al., 2001) and in this paper they have been compared to FP film measurements in order to assess their reliability in predicting the values of the

above mentioned mechanical and geometrical quantities. The advantages of FEM lie in their great flexibility, that means that many design parameters can be changed to predict how they can influence the mechanical behaviour of the prosthesis without prototyping new models, once the 3-D CAD files are available.

As regards the values of contact area the differences between FEM calculations and FP film measurements lie between -6% and 6% : the discrepancies between FEM and FP results are smaller than that reported by Liau et al. (2001), who found that the insertion of a FP film to measure contact areas in artificial tibiofemoral joints has the effect to overestimate the true contact area of about 20–25%.

As regards the prediction of the fatigue life of the TT, the use of FEM methods coupled with Sines' fatigue life criterion gave good results, in agreement with our in vitro tests. Indeed, results are very similar, the uncertainty depending once more on the interval where the fatigue limit of the material lies (the actual value of

σ_F was not available and had to be drawn from literature data). A limitation of the fatigue test of this study is the limited number of samples tested. We are aware that six samples are not sufficient to draw firm conclusions, but these preliminary results seems to be promising.

In conclusion, both computational and experimental methods play an important role in designing reliable prostheses. The former is useful in the evaluation of the initial designing phase where some parameters dealing with material properties, dimensions of components, structures and shapes of contacting surfaces have to be chosen. The latter finds its proper application in the validation phase where a final prototype, which includes shape, material and technological process, has to be tested.

References

- Abernethy, P.J., Robinson, C.M., Fowler, R.M., 1996. Fracture of the metal tibial tray after kinematic total knee replacement. A common cause of early aseptic failure. *Journal of Bone and Joint Surgery (British Volume)* 78, 220–225.
- Ahir, S.P., Blunn, G.W., Haider, H., Walker, P.S., 1999. Evaluation of a testing method for the fatigue performance of total knee tibial trays. *Journal of Biomechanics* 32, 1049–1057.
- Altintas, F., Sener, N., Ugutmen, E., 1999. Fracture of the tibial tray after total knee arthroplasty. *Journal of Arthroplasty* 14, 112–114.
- Baker, D.A., Hastings, R.S., Pruitt, L., 2000. Compression and tension fatigue resistance of medical grade ultra high molecular weight polyethylene: the effect of morphology, sterilization, aging and temperature. *Polymer* 41, 795–808.
- Bell, C.J., Walker, P.S., Sathasivam, S., Campbell, P.A., Blunn, G.W., 1999. Differences in wear between fixed bearing and mobile bearing knees. *Transaction of Orthopaedic Research Society* 24, 962.
- Blunn, G.W., Joshi, A.B., Minns, R.J., Lidgren, L., Lilley, P., Ryd, L., Engelbrecht, E., Walker, P.S., 1997. Wear in retrieved condylar knee arthroplasties. A comparison of wear in different designs of 280 retrieved condylar knee prostheses. *Journal of Arthroplasty* 12, 281–290.
- Buchalla, R., Schüttler, C., Bögl, K.W., 1995. Radiation sterilization of medical devices. Effects of ionizing radiation on ultra-high molecular-weight polyethylene. *Radiation Physics and Chemistry* 46, 579–585.
- Buechel, F.F., Pappas, M.J., 1990. Long-term survivorship analysis of cruciate-sparing versus cruciate-sacrificing knee prostheses using meniscal bearings. *Clinical Orthopaedic* 260, 162–169.
- Callaghan, J.J., Squire, M.W., Goetz, D.D., Sullivan, P.M., Johnston, R.C., 2000. Cemented rotating-platform total knee replacement. A nine to twelve-year follow-up study. *Journal of Bone and Joint Surgery* 82, 705–711.
- Chen, F., Krackow, K.A., 1994. Management of tibial defects in total knee arthroplasty. *Clinical Orthopaedics and Related Research* 305, 249–257.
- Flivik, G., Ljung, P., Rydholm, U., 1990. Fracture of the tibial tray of the PCA knee: a case report of early failure caused by improper design. *Acta Orthopaedica Scandinavica* 61, 26–28.
- Gradisar, I.A., Holman, M.L., Askew, M.J., 1989. Fracture of a fenestrated metal backing of a tibial knee component: a case report. *Journal of Arthroplasty* 4, 27–30.
- Harris, M.L., Morberg, P., Bruce, W.J.M., Walsh, W.R., 1999. An improved method for measuring tibiofemoral contact areas in total knee arthroplasty: a comparison of K-scan sensor and Fuji film. *Journal of Biomechanics* 32, 951–958.
- Jordan, L.R., Olivo, J.L., Voorhorst, P.E., 1997. Survivorship analysis of cementless meniscal bearing total knee arthroplasty. *Clinical Orthopaedic* 338, 119–123.
- Liau, J.-J., Hu, C.-C., Cheng, C.-K., Huang, C.-H., Lo, W.-H., 2001. The influence of inserting a Fuji pressure sensitive film between the tibiofemoral joint of knee prosthesis on actual contact characteristics. *Clinical Biomechanics* 16, 160–166.
- Maruyama, M., Terayama, K., Sunohara, H., Adachi, T., Suzuki, S., Fukuzawa, T., 1994. Fracture of the tibial tray following pca knee replacement. A report of two cases. *Archives of Orthopaedic and Trauma Surgery* 113 (6), 330–333.
- McNamara, J.L., Collier, J.P., Mayor, M.B., Jensen, R.E., 1994. A comparison of contact pressures in tibial and patellar total knee components before and after service in vivo. *Clinical Orthopaedics* 299, 104–113.
- Mendes, D.G., Brandon, D., Galor, L., Roffman, M., 1984. Breakage of the metal tray in total knee replacement. *Orthopaedics* 7, 860–862.
- Moreland, J.R., 1988. Mechanisms of failure in total knee arthroplasty. *Clinical Orthopaedics and Related Research* 226, 49–64.
- Morrey, B.F., Chao, E.Y.S., 1988. Fracture of the porous-coated metal tray of a biologically fixed knee prosthesis: report of a case. *Clinical Orthopaedics and Related Research* 228, 182–189.
- Morrison, J.B., 1970. The mechanics of muscle function in locomotion. *Journal of Biomechanics* 3, 431–451.
- Murray, D.W., Goodfellow, J.W., O'Connor, J.J., 1998. The Oxford medial unicompartmental arthroplasty: a ten-year survival study. *Journal of Bone and Joint Surgery* 80, 983–989.
- Otto, J.K., Callaghan, J.J., Brown, T.D., 2001. Mobility and contact mechanics of a rotating platform total knee replacement. *Clinical Orthopaedics and Related Research* 392, 24–37.
- Rose, R.M., Goldfarb, H.V., 1983. On the pressure dependence of the wear of ultra high molecular weight polyethylene. *Wear* 92, 99–111.
- Rostoker, W., Galante, J.O., 1979. Contact pressure dependence of wear rates of ultra high molecular weight polyethylene. *Journal of Biomedical Materials Research* 13, 957–964.
- Sathasivam, S., Walker, P.S., Campbell, P.A., Rayner, K., 2001. The effect of contact area on wear in relation to fixed bearing and mobile bearing knee replacements. *Journal of Biomedical and Material Research* 58, 282–290.
- Scott, R.D., Ewald, F.C., Walker, P.S., 1984. Fracture of the metal tray following total knee replacement. *Journal of Bone and Joint Surgery* 66, 780–782.
- Sines, G., 1959. In: Sines, G., Waisman, J.L. (Eds.), *Behaviour of Metals Under Complex Stating and Alternating Stresses*, in *Metal Fatigue*. McGraw Hill, New York.
- Sorrells, R.B., 1996. The rotating platform mobile bearing TKA. *Orthopedics* 19, 793–796.
- Stiehl, J.B., Dennis, D.A., Komistek, R.D., Keblish, P.A., 1997. In vivo kinematic analysis of a mobile bearing total knee prosthesis. *Clinical Orthopaedics* 345, 60–66.
- Svard, U.C., Price, A.J., 2001. Oxford medial unicompartmental knee arthroplasty. A survival analysis of an independent series. *Journal of Bone and Joint Surgery (British Volume)* 83, 191–194.
- Szivek, J.A., Cutignola, L., Volz, R.G., 1995. Tibiofemoral contact stress and stress distribution evaluation of total knee arthroplasties. *Journal of Arthroplasty* 10, 480–491.
- Wasielewski, R.C., Galante, J.O., Leighty, R.M., Natarajan, R.N., Rosenberg, A.G., 1994. Wear patterns on retrieved polyethylene tibial inserts and their relationship to technical considerations during total knee arthroplasty. *Clinical Orthopaedic* 299, 31–43.
- Yang, R.S., Lin, H.J., 2001. Contact stress on polyethylene components of a new rotating hinge with a spherical contact surface. *Clinical Biomechanics* 16, 540–546.